
**PHYSICS OF EARTH, ATMOSPHERE,
AND HYDROSPHERE**

**Numerical Simulation of the Effect of Wind on the Transport
of Contaminants in the Selenga Shallow Waters of Lake Baikal
during the Autumnal Thermal Bar**

B. O. Tsydenov*

*Computational Geophysics Laboratory, Faculty of Mechanics and Mathematics, Tomsk State University,
Tomsk 634050, Russia*

Received September 9, 2019; revised October 14, 2019; accepted October 14, 2019

Abstract—The results of the mathematical simulation of contaminant transport in the Selenga shallow waters of Lake Baikal during the development of the autumnal thermal bar are presented. Spatial distribution of contaminants under different wind scenarios are analyzed. Numerical experiments showed that the structure of the contour lines of the contaminant concentration depends on the wind direction when shallow waters cool.

Keywords: water contamination, numerical simulation, autumnal thermal bar, wind mixing, Selenga shallow waters, Lake Baikal.

DOI: 10.3103/S0027134920010142

INTRODUCTION

A thermal bar (a natural phenomenon that consists of a narrow zone of water sinking at the temperature of maximum density [1, 2]) in Lake Baikal forms in straits and bays (the Maloye More strait and the Chivyrkuy bay), shallow waters (the Selenga shallow waters), and near relatively shallow coastal areas [3]. In the Selenga shallow waters, temperature contrasts between river and lake waters are constantly observed, which cause thermal convection and thermal bars to occur [4]. In addition, the hydrooptical characteristics of the waters of the Selenga River differ sharply from those of Lake Baikal [5].

The wind plays the most important role in the hydrodynamics of the thermal bar [6–8], especially during autumn cooling of the water body [9, 10]. The wind can shift the convergence zone relative to isotherm 4°C on the surface of the lake or completely destroy the front of the thermal bar [11, 12]. The variable (in direction and force) wind effect on the water body is explained by the variable current regime in the Selenga shallow waters of Lake Baikal [13].

It is known that the thermal bar in large lakes serves as a barrier that limits the spread of coastal waters with high concentrations of contaminants and biota to the central part [14–16]. At the same time, vertical fluxes formed by thermobaric instability can

contribute to the transport of contaminants to the deep area of the water body [2, 17]. Convective and dynamic processes in the Selenga shallow waters during the thermal bar lead to the fact that suspended and dissolved substances of natural and anthropogenic origin enter the lake in a well-mixed form [4]. The front of the thermal bar in the Selenga shallow waters is a clear boundary between yellowish coastal and transparent lake waters [13].

The purpose of this article was to numerically study the effect of wind on the specific distribution of contaminants in the Selenga shallow waters of Lake Baikal during the autumnal thermal bar.

1. MATHEMATICAL MODEL

1.1. Governing Equations of the Model

This article considers an area $L_x = 10$ km long and $L_z = 66$ m deep, which is a vertical section in the area of the Selenga River inflow into Lake Baikal (Fig. 1). The problem is solved in the Ox, Oy, Oz coordinate system (the origin coincides with the river mouth). The Ox axis is directed to the center of the lake, Oy is directed along the shore, and Oz is directed vertically upward (Fig. 1).

The nonhydrostatic 2.5D model to reproduce the processes of contaminant proliferation in a freshwater lake includes the following equations:

*E-mail: tsydenov@math.tsu.ru

1. Contaminant concentration equation

$$\begin{aligned} & \frac{\partial C}{\partial t} + \frac{\partial uC}{\partial x} + \frac{\partial wC}{\partial z} \\ &= \frac{\partial}{\partial x} \left(D_x \frac{\partial C}{\partial x} \right) + \frac{\partial}{\partial z} \left(D_z \frac{\partial C}{\partial z} \right); \end{aligned} \quad (1)$$

2. Momentum equation

$$\begin{aligned} \frac{\partial u}{\partial t} + \frac{\partial u^2}{\partial x} + \frac{\partial uw}{\partial z} &= -\frac{1}{\rho_0} \frac{\partial p}{\partial x} + \frac{\partial}{\partial x} \left(K_x \frac{\partial u}{\partial x} \right) \\ &+ \frac{\partial}{\partial z} \left(K_z \frac{\partial u}{\partial z} \right) + 2\Omega_z v - 2\Omega_y w; \end{aligned} \quad (2)$$

$$\begin{aligned} \frac{\partial v}{\partial t} + \frac{\partial uv}{\partial x} + \frac{\partial vw}{\partial z} &= \frac{\partial}{\partial x} \left(K_x \frac{\partial v}{\partial x} \right) \\ &+ \frac{\partial}{\partial z} \left(K_z \frac{\partial v}{\partial z} \right) + 2\Omega_x w - 2\Omega_z u; \end{aligned} \quad (3)$$

$$\begin{aligned} \frac{\partial w}{\partial t} + \frac{\partial uw}{\partial x} + \frac{\partial w^2}{\partial z} &= -\frac{1}{\rho_0} \frac{\partial p}{\partial z} + \frac{\partial}{\partial x} \left(K_x \frac{\partial w}{\partial x} \right) \\ &+ \frac{\partial}{\partial z} \left(K_z \frac{\partial w}{\partial z} \right) - \frac{g\rho}{\rho_0} + 2\Omega_y u - 2\Omega_x v; \end{aligned} \quad (4)$$

3. Continuity equation

$$\frac{\partial u}{\partial x} + \frac{\partial w}{\partial z} = 0; \quad (5)$$

4. Energy equation

$$\begin{aligned} \frac{\partial T}{\partial t} + \frac{\partial uT}{\partial x} + \frac{\partial wT}{\partial z} &= \frac{\partial}{\partial x} \left(D_x \frac{\partial T}{\partial x} \right) \\ &+ \frac{\partial}{\partial z} \left(D_z \frac{\partial T}{\partial z} \right) + \frac{1}{\rho_0 c_p} \frac{\partial H_{\text{sol}}}{\partial z}; \end{aligned} \quad (6)$$

5. Mineralization equation

$$\begin{aligned} \frac{\partial S}{\partial t} + \frac{\partial uS}{\partial x} + \frac{\partial wS}{\partial z} \\ &= \frac{\partial}{\partial x} \left(D_x \frac{\partial S}{\partial x} \right) + \frac{\partial}{\partial z} \left(D_z \frac{\partial S}{\partial z} \right), \end{aligned} \quad (7)$$

where C is the contaminant concentration; u , v are horizontal velocity components; w is the vertical velocity component, Ω_x , Ω_y , and Ω_z are components of the Earth's angular velocity vector; g is the free fall acceleration; c_p is the specific heat capacity; T is the temperature; S is the salinity; p is the pressure; and ρ_0 is the maximum density of pure water (999.975 kg/m³).

Solar radiation absorption H_{sol} is calculated by the Beer–Lambert–Bouguer law:

$$H_{\text{sol}} = H_{S_{\text{sol},0}} (1 - r_s) \exp(-\epsilon_{\text{abs}} d), \quad (8)$$

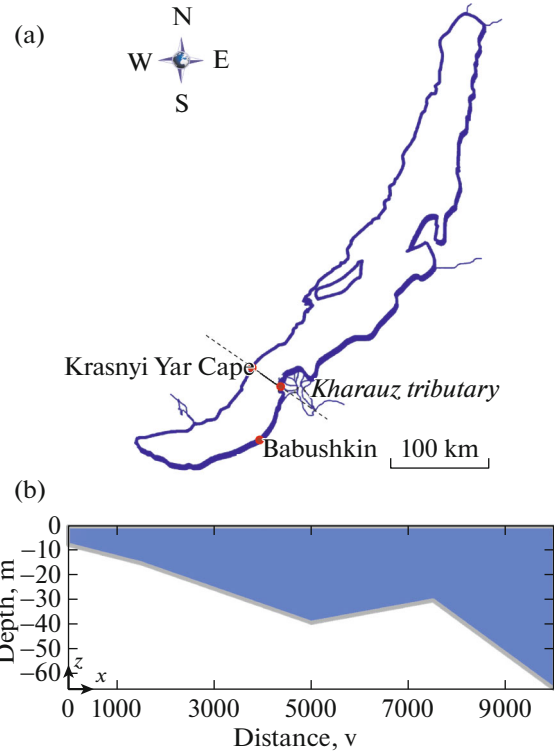


Fig. 1. The Kharauz tributary–Krasnyi Yar Cape section: (a) section diagram and (b) calculation area.

where $H_{S_{\text{sol},0}}$ is the flux of short-wave (solar) radiation on the surface of a water body [17, 18]; $r_s \approx 0.2$ is the water reflection coefficient; $\epsilon_{\text{abs}} \approx 0.3 \text{ m}^{-1}$ is the absorption coefficient of solar radiation in water; and $d = |L_z - z|$ is the depth, m.

The density of water is calculated by the Chen–Millero formula [19]. The diffusion transport rate of impulse and heat are determined based on the k – ω model of turbulence [20].

1.2. Initial and Boundary Conditions

Initial conditions (for $t = 0$) for the model equations are as follows

$$\begin{aligned} u &= 0; \quad v = 0; \quad w = 0; \quad C = 0; \\ T &= T_L(z); \quad S = S_L, \end{aligned} \quad (9)$$

where $T_L(z)$ and S_L are the temperature and salinity of the water in the lake, respectively, and t is the time.

The boundary conditions are specified as follows

1. At the water–air interface

$$\begin{aligned} K_z \frac{\partial u}{\partial z} &= \frac{\tau_{\text{surf}}^u}{\rho_0}; \quad K_z \frac{\partial v}{\partial z} = \frac{\tau_{\text{surf}}^v}{\rho_0}; \quad w = 0; \\ \frac{\partial C}{\partial z} &= 0; \quad D_z \frac{\partial T}{\partial z} = \frac{H_{\text{net}}}{\rho_0 c_p}; \quad \frac{\partial S}{\partial z} = 0, \end{aligned} \quad (10)$$

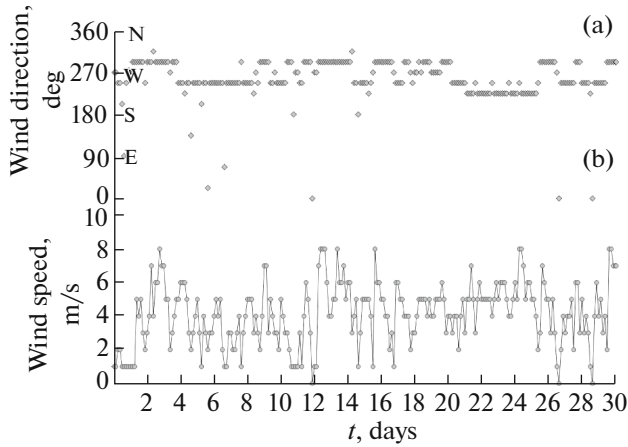


Fig. 2. The direction (a) and speed (b) of the wind according to the data of the Babushkin meteorological station from November 1 to November 30, 2015.

where H_{net} is the heat flux, which includes components of longwave radiation, as well as the latent and sensible heat. The shear stress of wind on the surface of the lake is described by the law

$$\tau_{\text{surf}}^u = c_{10} \rho_a \sqrt{u_{10}^2 + v_{10}^2} \cdot u_{10};$$

$$\tau_{\text{surf}}^v = c_{10} \rho_a \sqrt{u_{10}^2 + v_{10}^2} \cdot v_{10},$$

Here, ρ_a is the air density at the water surface; u_{10} , v_{10} is the wind speed at 10 m above the lake surface; $c_{10} = 1.3 \times 10^{-3}$;

2. *At solid boundaries (at the bottom)*

$$u = 0; \quad v = 0; \quad w = 0;$$

$$\frac{\partial C}{\partial n} = 0; \quad \frac{\partial T}{\partial n} = 0; \quad \frac{\partial S}{\partial n} = 0, \quad (11)$$

where n is the direction of the external normal to the area;

3. *At the river–lake interface*

$$u = u_R; \quad v = 0; \quad w = 0; \quad C = C_R;$$

$$T = T_R; \quad S = S_R, \quad (12)$$

where u_R is the velocity of inflow into the river mouth; C_R , T_R , and S_R are the concentration of contaminants, as well as the temperature and salinity of the water in the river, respectively;

4. *At the open boundary* the radiation conditions [21] and simple gradient conditions are specified

$$\frac{\partial \phi}{\partial t} + c_\phi \frac{\partial \phi}{\partial x} = 0 \quad (\phi = u, v, C, T, S);$$

$$\frac{\partial w}{\partial x} = 0. \quad (13)$$

2. THE AREA OF RESEARCH AND PARAMETERS OF THE PROBLEM

The Selenga shallow waters are between 51.9° – 52.5° N and 106.1° – 106.9° E. Geometrically, this is a cone formed by the accumulation of sediment [22]. The area of research is the cross-section in the area of the Selenga River inflow into Lake Baikal: Kharauz tributary–Krasnyi Yar Cape (Fig. 1a). Data on the bottom relief corresponding to the specified section were taken from [23].

The computational area is 10 km long and 66 m deep (Fig. 1b). The depth of the open section of the river runoff (at the left boundary) is 7.5 m. The calculation area is covered by a uniform orthogonal grid with spacings of $h_x = 12.5$ m and $h_z = 1.5$ m. The time step is 60 s.

The vertically inhomogeneous distribution of water temperature adopted in the model approximates the average annual values in the southern basin of Lake Baikal in October [24]. The water temperature of the river inflow uniformly decreases from 2 to 1°C , which reflects real thermal regime of the Kharauz tributary during the modeled period [4]. Mineralization of water in the lake is 96 mg/kg [24]. In the river, it varies from 185 to 200 mg/kg [4]. The inflow velocity of the Kharauz tributary into Lake Baikal is assumed to be 0.2 cm/s [25]. Components of heat fluxes that arrive at the water mirror are calculated according to the formulas given in [26] based on data on air temperature, relative humidity, atmospheric pressure, cloudiness, and wind speed (Fig. 2) obtained from the archive of weather conditions of the Babushkin weather station from November 1 to November 30, 2015. The value of the contaminant concentration in the river mouth is set to 1 g/m^3 .

The section of the Kharauz tributary–Krasnyi Yar Cape corresponds to the geographical latitude of 52.25° , and the angle of section with respect to the east is 150° .

3. SIMULATION RESULTS

A numerical study of the thermal bar dynamics at the Selenga shallow waters of Lake Baikal in November 2015 was described in detail in [27]. This article presents the results on the distribution of the contaminant concentration obtained under different wind scenarios during the autumnal thermal bar.

In the period from November 1 to November 30, 2015, west winds were prevailing, among which west-northwest winds were the longest in the first decade of the month, west-northwest winds were the longest in the second decade, and southwest winds were the longest in the third decade (Fig. 2a). These data are in agreement with the data of average annual observations during the periods when the lake is free

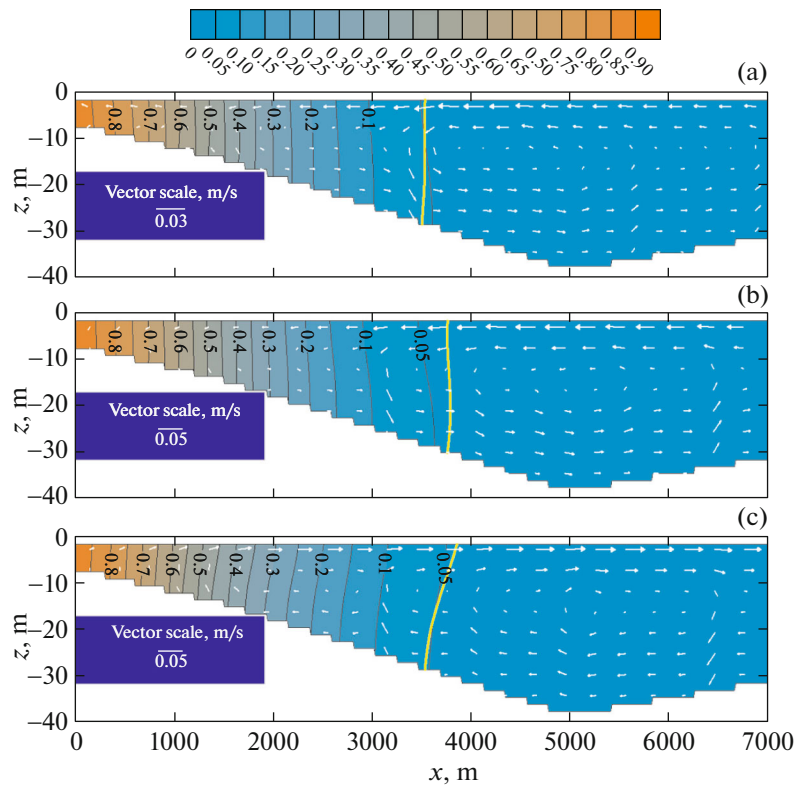


Fig. 3. The contaminant concentration distribution [g/m^3], velocity vector field, and maximum density temperature profile (bold line) after 16 days of modeling: (a) for real wind conditions, (b) for westerly wind blowing at 8 m/s, and (c) for easterly wind blowing at 8 m/s.

from ice [24], including during the spring thermal bar in May 2015 [8]. The mean value of the wind speed in the considered time interval was 4.1 m/s, which is lower than the data of observations over the surface of Southern Baikal and nearby areas for the same month (5.2 m/s) and higher than the mean annual value (4.0 m/s) [13, 24]. The maximum wind speed value was 8 m/s (Fig. 2b). The weather conditions and variation of short- and longwave radiation fluxes, as well as the sensible and latent heat, were described in detail in [27].

After 16 days of modeling, the thermal bar was at a distance of 3.5 km from the river mouth [27]. Despite the formation of a continuous jet on the surface of the water body (directed to the river mouth) due to the wind-induced wave, the front of the thermal bar had a pronounced zone with sinking of water masses (Fig. 3a). The maximum speed of the vertical flow inside the thermal bar front was 1.5 cm/s and the speed of wind-generated surface currents reached 2.0 cm/s. Due to wind mixing, the concentration of contaminants in shallow waters has a fairly uniform depth distribution (contour lines are predominantly vertical) (Fig. 3a). A similar vertical structure of contour lines was observed for the temperature field (Fig. 4c in [27]). As the distance from the shore increased, the

concentration of contaminants in shallow waters decreased. The results of the simulation are consistent with the descriptions of field observations: the thermal bar sequentially fills the Selenga shallow waters with water mixed by isobaths toward a depth increase [4]. On day 16, the 30 concentration of contaminants had spread up to 2 km from the river mouth (Fig. 3a).

In order to assess the effect of wind direction on the contaminant transport in shallow water conditions, additional calculations with the following wind characteristics were carried out along with the basic modeling (reflecting the real wind conditions in November 2015):

1. the west wind blowing at a speed of 8 m/s (computational experiment no. 1);
2. the east wind blowing at a speed of 8 m/s (computational experiment no. 2).

The distributions obtained during computational experiment no. 1 (Fig. 3b) do not significantly differ from the results of the basic modeling, because in the cases under consideration the wind is directed against the movement of the thermal bar. However, it should be noted that the contour lines of the contaminant concentration in experiment no. 1 are slightly shifted

toward the shore and have a greater slope in the near-surface layer and the slope angle increases with increasing distance from the river mouth (Fig. 3b). This difference is related to the wind force (in experiment no. 1 the wind speed is constant and coincides with the maximum value recorded in November 2015). By comparing the simulated distributions (Figs. 3a and 3b) we can conclude that the western winds delay the spread of contaminants into the central part of the water body.

If the wind blows in the direction of the thermal bar development (experiment no. 2), the reverse situation is observed: the contour lines of the contaminant concentration have a slope in the opposite direction (to the open part of the lake) (Fig. 3b). This indicates that the winds of the eastern direction contribute to a faster spread of contaminants in the upper layers of the water body. In the surface layer of the shallow waters, the 5% concentration of contaminants on day 16 in experiment no. 1 reached a distance of 3.45 km (Fig. 3b) and in experiment no. 2, 3.75 km (Fig. 3b). In the part of the shallow waters near the river mouth, the role of wind in contaminant distribution was insignificant due to the dominant effect of river runoff.

In the case of a continuous effect of wind on a water body, the large-scale circulation in the area of $3 < x < 6.5$ km (the maximum horizontal velocity of water in the circulation structure near the surface was 4 cm/s) is formed: in experiment no. 1 it is directed counter-clockwise and in experiment no. 2, in the opposite direction (Figs. 3b and 3c). In this case, the maximum density temperature region in both cases (in contrast to the basic scenario) is shifted toward the open lake. In experiments no. 1 and no. 2, vertical movements of water masses are not observed in the areas with the temperature of maximum density.

The performed mathematical simulation showed that the concentration of contaminants in the section of the Kharauz tributary–Krasnyi Yar Cape has a more uniform vertical distribution due to wind mixing in comparison with previously obtained results for the spring thermal bar [17, 28].

CONCLUSIONS

The conducted numerical simulation makes it possible to draw the following conclusions about the processes of contaminant transport in the Selenga shallow waters of Lake Baikal during the autumnal thermal bar:

1. The thermal and hydrodynamic regime of the Selenga River has a dominant effect on contaminant transport in the shallow waters near the river mouth.
2. As the distance from the river mouth increases, the effect of wind friction on the spatial distribution of the contaminant concentration also increases.
3. West winds blowing against the thermal bar movement lead to a delay in contaminant transport to the central part of the water body.
4. East winds contribute to faster distribution of contaminants in the upper layers of the water column.

ACKNOWLEDGMENTS

This work was supported by the Russian Science Foundation, project no. 18-77-00017.

REFERENCES

1. A. I. Tikhomirov, *Thermics of Large Lakes* (Nauka, Leningrad, 1982) [in Russian].
2. N. S. Blokhina and K. V. Pokazeev, *Zemlya Vsel.*, No. 6, 78 (2015).
3. M. N. Shimaraev, *Elements of the Thermal Regime of Lake Baikal* (Nauka, Novosibirsk, 1977) [in Russian].
4. P. P. Sherstyankin, V. G. Ivanov, L. N. Kuimova, and V. N. Sinyukovich, *Water Resour.* **34**, 408 (2007).
<https://doi.org/10.1134/S0097807807040057>
5. P. P. Sherstyankin, *Elements of the Hydrometeorological Regime of Lake Baikal*, Vol. 5 (25) of *Works of Limnol Inst., Acad. Sci. USSR, Sib. Dep.* (Moscow, Leningrad, 1964), p. 29 [in Russian].
6. N. S. Blokhina, *Moscow Univ. Phys. Bull.* **68**, 324 (2013).
<https://doi.org/10.3103/S0027134913040048>
7. J. Malm, *Nordic Hydrol.* **26**, 331 (1995).
<https://doi.org/10.2166/nh.1995.0019>
8. B. O. Tsydenov, A. V. Starchenko, and A. Kay, *Inland Waters* **8**, 322 (2018).
<https://doi.org/10.1080/20442041.2018.1481667>
9. D. Ullman, J. Brown, P. Cornillon, and T. Mavor, *J. Great Lakes Res.* **24**, 753 (1998).
[https://doi.org/10.1016/S0380-1330\(98\)70860-3](https://doi.org/10.1016/S0380-1330(98)70860-3)
10. B. O. Tsydenov, *Moscow Univ. Phys. Bull.* **74**, 70 (2019).
<https://doi.org/10.3103/S0027134919010156>
11. N. S. Blokhina, *Moscow Univ. Phys. Bull.* **70** (4), 102 (2015).
<https://doi.org/10.3103/S0027134915040050>
12. B. O. Tsydenov, *J. Mar. Syst.* **179**, 1 (2018).
<https://doi.org/10.1016/j.jmarsys.2017.11.004>
13. V. G. Ivanov, "Formation and evolution of a spring thermal bar due to river runoff (on the example of the Selenginsky shallow water of Lake Baikal)," *Cand. Sci. (Geogr.) Dissertation* (Irkutsk, 2012).

14. R. A. Moll, A. Bratkovich, W. Y. B. Chang, and P. Pu, *Estuaries* **16**, 92 (1993).
<https://doi.org/10.2307/1352767>
15. Y. V. Likhoshway, A. Ye. Kuzmina, T. G. Potyemkina, et al., *J. Great Lakes Res.* **22**, 5 (1996).
[https://doi.org/10.1016/S0380-1330\(96\)70929-2](https://doi.org/10.1016/S0380-1330(96)70929-2)
16. B. O. Tsydenov, *J. Mar. Syst.* **195**, 38 (2019).
<https://doi.org/10.1016/j.jmarsys.2019.03.009>
17. B. O. Tsydenov, A. Kay, and A. V. Starchenko, *Ocean Model.* **104**, 73 (2016).
<https://doi.org/10.1016/j.ocemod.2016.05.009>
18. B. O. Tsydenov and A. V. Starchenko, *Proc. SPIE* **9680**, 96800H (2015).
<https://doi.org/10.1117/12.2205687>
19. C. T. Chen and F. G. Millero, *Limnol. Oceanogr.* **31**, 657 (1986).
<https://doi.org/10.4319/lo.1986.31.3.0657>
20. D. C. Wilcox, *AIAA J.* **26**, 1299 (1988).
<https://doi.org/10.2514/3.10041>
21. I. Orlanski, *J. Comput. Phys.* **21**, 251 (1976).
[https://doi.org/10.1016/0021-9991\(76\)90023-1](https://doi.org/10.1016/0021-9991(76)90023-1)
22. V. N. Sinyukovich, N. G. Zharikova, and V. D. Zharikov, *Geogr. Prirod. Resursy*, No. 3, 64 (2004).
23. E. N. Tarasova, *Organic Matter of the Waters of South Baikal* (Nauka, Novosibirsk, 1975) [in Russian].
24. M. N. Shimaraev, V. I. Verbolov, N. G. Granin, and P. P. Sherstyankin, *Physical Limnology of Lake Baikal: A Review* (Irkutsk–Okayama, 1994).
25. V. I. Verbolov, *Lake Baikal Problems* (Nauka, Novosibirsk, 1978), p. 87 [in Russian].
26. B. O. Tsydenov, *Moscow Univ. Phys. Bull.* **73**, 435 (2018).
<https://doi.org/10.3103/S0027134918040148>
27. B. O. Tsydenov, *J. Great Lakes Res.* **45**, 715 (2019).
<https://doi.org/10.1016/j.jglr.2019.05.012>
28. B. O. Tsydenov, *Vychisl. Tekhnol.* **22** (S1), 113 (2017).

Translated by O. Pismenov